Heat and Fluid Flow Processes During the Coating of a Moving Surface

A. Rezaian* and D. Poulikakos†
University of Illinois at Chicago, Chicago, Illinois 60680

In this paper, a theoretical study is presented for the problem of coating a flat moving surface with a small Prandtl number melt, exemplified by a liquid metal or a liquid crystal. From the heat and fluid flow standpoint, the process is modeled as one of forced convection in the melt (induced by both the motion of the surface and the velocity of the melt as it is deposited on the surface) coupled with conduction in the solidifying coating layer. The effect of the main parameters of the problem, such as the ratio of the melt deposition velocity to the surface velocity, the Stefan number, the Prandtl number, and the ratios of the main properties of the solid and liquid phases on the thickness of the resulting coating layer and the heat transfer to the moving surface, are determined. An important assumption adopted in this study is that the moving surface is isothermal. The parametric domain of validity of this assumption is defined.

Nomenclature

A, B = dimensionless groups, Eqs. (15) and (31), respectively
c = specific heat of liquid phase
c_s = specific heat of solid phase
$\mathrm{erf}(x)$ = error function, $= (2/\sqrt{\pi}) \int_0^x e^{-\sigma^2}\, d\sigma$
$f(\xi)$ = similarity stream function
G = latent heat of fusion
k = thermal conductivity of liquid phase
k_s = thermal conductivity of solid phase
L = reference length
Nu = Nusselt number
Pr = Prandtl number
Re_L = Reynolds number based on a reference length L, $= U_w L/\nu$
Re_{x_*} = Reynolds number based on x_*, $= U_w x_*/\nu$
Ste = Stefan number
T = dimensionless temperature in the liquid phase
T_{b_*} = temperature of the body on which the coating is deposited
T_f = freezing temperature
T_{s_*} = temperature of the solid phase
T_s = dimensionless temperature in the solid phase
T_w = wall temperature
$\bar{T}_w$ = average wall temperature used in the scaling arguments of the Appendix
T_0 = body temperature outside the thermal boundary layer
T_∞ = freestream temperature of the melt
U_w = velocity of the surface
U_∞ = freestream velocity of the melt
u = dimensionless velocity component in the x direction
v = dimensionless velocity component in the y direction
x, y = Cartesian coordinates
α = thermal diffusivity in the liquid phase
α_b = thermal diffusivity of the body on which the coating is deposited
α_s = thermal diffusivity in the solid phase
Δ = displacement thickness
δ = thermal boundary-layer thickness scale in the body
δ_s = dimensionless thickness of the coating layer
ν = viscosity in the liquid phase
ξ = similarity variable
ξ_s = similarity variable evaluated at the solidification interface
ρ = density of liquid phase
ρ_s = density of solid phase
ψ = stream function

Subscript

* = denoting dimensional quantity

Superscript

′ = denoting differentiation with respect to ξ

Received Oct. 20, 1989; revision received Feb. 1, 1990.

*Graduate Student, Mechanical Engineering Department.
†Associate Professor, Mechanical Engineering Department.

I. Introduction

SOLIDIFICATION on moving surfaces has direct engineering applications exemplified by coating processes and ribbon or fiber growth processes. With reference to the former, a liquid metal or liquid crystal is often deposited on a moving chilled surface (also termed the substrate) with the purpose of coating that surface with a solid layer of desired thickness. With reference to the latter, several techniques aiming at the production of thin strip-type materials involve deposition of a melt of a metal-metalloid or a melt of a metglass on a cold moving surface. Examples of such techniques are melt spinning, twin roller quenching, melt extraction, and pendant drop.[1]

Despite the importance of these applications, several questions related to the role of heat transfer and fluid flow during the growth of the solid layer remain unanswered. Here, we will briefly review representative studies from the related work existing in the heat transfer literature.

Kuiken[2] investigated the growth of a solid layer on an isothermal cold sheet moving through a warm liquid bath. Asymptotic expressions were reported for the solid thickness in special cases. Approximate solutions of the energy equation at small Prandtl numbers were also obtained by replacing the velocity field in the energy equation with the asymptotic freestream velocity field.

Using an integral method, Griffin[3] studied the problem of contact melting of solids on a hot moving surface. His study applies to polymer melting in extruders. Levy et al.[4] examined the heat transfer process during the freeze coating of fibers. They neglected convective effects and modeled the freeze-coating process as a diffusion, Stefan-type problem. These

authors also used Deryagin's viscous-coating theory[5] to estimate the viscous deposition of the melt onto the moving fiber.

The coating of amorphous metal ribbons by melt extraction was investigated by Anthony and Cline[6] with the help of simplifying assumptions. They obtained the viscous shear-layer thickness around a rotating cylinder and used it as the lower limit for the solidified ribbon thickness. Their work did not include a fundamental heat transfer analysis of the solidification process on the moving cold surface. Zoutendyk[7] analyzed the convective heat transfer process in the horizontal ribbon growth (HRG) of semiconductor crystals. He concluded that for successful growth of crystal ribbons active cooling was necessary at the growth tip region. Closed-form expressions for the freeze-coat thickness of a molten polymeric substance at its fusion temperature on a moving cylinder or plate were reported by Seeniraj and Bose.[8]

Cheung[9] extended the analysis of Seeniraj and Bose[8] to the freeze coating of a superheated polymeric liquid on a non-isothermal moving plate. He modeled the convective heat transfer at the solid-liquid interface by treating the heat transfer coefficient as an known parameter. To this end, he used the heat transfer coefficient that was valid for the laminar boundary-layer heat transfer on a moving plate at large Prandtl numbers (Erickson et al.[10,11]). Cheung[9] allowed for the axial variation of the plate temperature and identified the parameters controlling the solution. In a later paper, Cheung[12] examined the freezing process on a thick moving plate by a similarity analysis. He assumed a constant temperature at the interface between the freeze coat and the plate and numerically determined the local convective heat transfer coefficient and the axial variation of the solid-layer thickness as functions of the system parameters. He concluded that, due to the interaction between the phase-change process and the flow, the local heat transfer coefficient at the freezing front is larger than that of the forced flow on a moving plate without freezing.

Cheung and Cha[13] carried out a numerical study of the freeze-coating process on a continuous moving cylinder by a finite difference method. The cylinder temperature was allowed to vary in both axial and radial directions. Existing results for convective heat transfer to moving cylinders were utilized to approximate the heat convection from the liquid to the freeze coat, i.e., the convection problem in the liquid was not solved simultaneously with the conduction problem in the coating layer and the cylinder. Growth and decay behavior of the freeze coat was observed and the maximum attainable thickness was determined for various conditions.

The present study aims at investigating the process of deposition of a coating of small Prandtl number material (liquid metal or liquid glass, for example) on a flat moving isothermal surface (substrate). The arrangement relevant to this study is shown schematically in Fig. 1a, and it has been used for coating applications and ribbon growth of glass and metallic strips. As shown in Fig. 1a, upon deposition of the material on the moving surface, backflow and rippling effects at the surface of the liquid usually occur. As a result, instabilities may take place that cause imperfections at the coating layer surface and make the control and prediction of its thickness inaccurate. To circumvent these deficiencies, we propose the arrangement shown in Fig. 1b. In this arrangement, the deposited molten material flows parallel to the moving substrate. The modeling and analysis of the configuration in Fig. 1b is the main contribution of the present study.

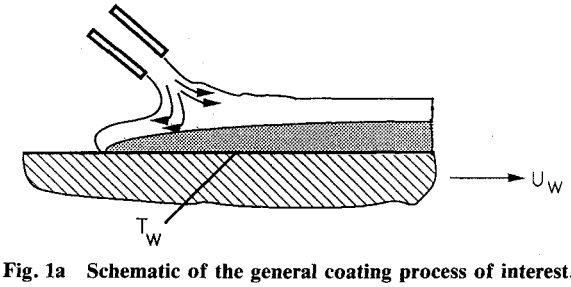

Fig. 1a Schematic of the general coating process of interest.

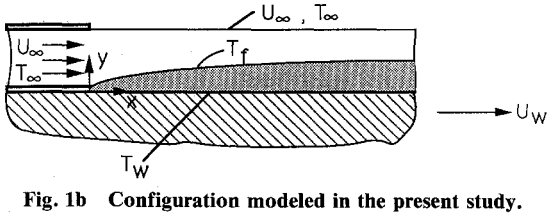

Fig. 1b Configuration modeled in the present study.

II. Mathematical Formulation

The problem is defined schematically in Fig. 1b. The coating material (liquid metal or liquid glass) exits as a rectangular slot with uniform velocity U_∞ and temperature T_∞. Immediately after exiting, the coating material is deposited on a substrate (flat surface) moving with velocity U_w. The temperature of the flat surface is denoted by T_w, is assumed constant, and is considerably lower than the temperature of the liquid metal T_∞, i.e., $T_w < T_\infty$. As a result, solidification of the melt takes place and the coating layer shown in Fig. 1b is created. The assumption of a constant surface temperature T_w is adopted with the understanding that the present is a basic study of the phenomenon of interest. It is worthwhile, however, to define the parametric domain in which this assumption will be valid in a real coating application. A scaling analysis is performed with this purpose and is reported in the Appendix. In addition, the present work pertains to applications in which the substrate upon which the coating is deposited is continuously cooled[1] or has a thermal capacity considerably larger than that of the coating layer. Therefore, the substrate temperature (in the lengthwise direction, for example) remains essentially constant and is not markedly altered by the heat the solidifying material releases.

Clearly, to analyze this problem from the standpoint of heat transfer and fluid mechanics, forced convection in the liquid phase and conduction in the solidified coating layer need to be considered simultaneously. In formulating the problem mathematically, the following assumptions are made.

1) All thermophysical properties are constant.

2) The flow is of the boundary-layer type: steady and laminar.

3) The phase-change process is steady and takes place at a constant temperature T_f. The solidification front is sharp and planar, and thermal equilibrium exists at the interface.

4) The solid layer is thin enough so that its curvature does not affect the flowfield.

5) Axial heat conduction in the coating is negligible.

6) The shear stress effect at the free surface of the liquid region is negligible.

Assumption 4 allows for the modeling of the flow and heat transfer in the liquid region as forced convection from a flat plate with suction, the suction being provided by the solidification interface. It is through this suction that the convection in the liquid phase is coupled with the conduction in the coating layer. Based on the previous assumptions, the dimensionless equations governing the conservation of mass momentum and heat transport in the system of interest with respect to the Cartesian coordinate systems of Fig. 1b are the following:

Liquid Region

$$\frac{\partial u}{\partial x} + \frac{\partial v}{\partial y} = 0 \tag{1}$$

$$u\frac{\partial u}{\partial x} + v\frac{\partial v}{\partial y} = \frac{\partial^2 u}{\partial y^2} \tag{2}$$

$$u\frac{\partial T}{\partial x} + v\frac{\partial T}{\partial y} = \frac{1}{Pr}\frac{\partial^2 T}{\partial y^2} \tag{3}$$

Solid Region

$$\frac{\partial^2 T_s}{\partial y^2} - Pr\, A \frac{\partial T_s}{\partial x} = 0 \tag{4}$$

To complete the formulation of the problem, the boundary conditions and the matching conditions at the solid/liquid interface are stated next.

At the moving surface ($y = 0$):

$$T_s(x, 0) = 0 \tag{5}$$

$$\delta_s(0,0) = 0 \tag{6}$$

At the solidifying interface ($y = 0$ or $y = \delta_s$):

$$u(x,\delta_s) = 1 \tag{7}$$

$$v(x, \delta_s) = \left(1 - \frac{\rho_s}{\rho}\right)\frac{d\delta_s}{dx} \tag{8}$$

$$T_s(x, \delta_s) = 1 \tag{9}$$

$$T(x, 0) = 1 \tag{10}$$

$$\frac{d\delta_s}{dx} = \frac{Ste}{PrA}\left[\left(\frac{\partial T_s}{\partial y}\right)_{y=\delta_s} + \frac{k}{k_s}\frac{T_f - T_\infty}{T_w - T_f}\left(\frac{\partial T}{\partial y}\right)_{y=\delta_s}\right] \tag{11}$$

Outside the thermal boundary layer ($y \to \infty$):

$$u(x, y \to \infty) = U_\infty / U_w \tag{12}$$

$$T(x, y \to \infty) = 0 \tag{13}$$

The dimensionless variables appearing in Eqs. (1–13) are defined as follows:

$$x = \frac{x_*}{L}, \quad y = \frac{y_*}{LRe_L^{-1/2}}, \quad \delta_s = \frac{\delta_{s_*}}{Re_L^{-1/2}L}, \quad u = \frac{u_*}{U_w},$$

$$v = \frac{v_*}{U_w Re_L^{-1/2}}, \quad T = \frac{T_* - T_\infty}{T_f - T_\infty}, \quad T_s = \frac{T_{s_*} - T_w}{T_f - T_w} \tag{14}$$

In addition to Eqs. (14), the nondimensionalization yielded the following groups:

$$Re_L = \frac{U_w L}{\nu}, \quad Pr = \frac{\nu}{\alpha}, \quad A = \frac{\alpha}{\alpha_s}, \quad Ste = \frac{c_s(T_f - T_w)}{G} \tag{15}$$

These groups are the Reynolds number, Prandtl number, the ratio of liquid to solid thermal diffusivity, and the Stefan number, respectively. Most of the boundary conditions are self explanatory. However, it is worth noting that Eq. (8) represents a mass balance at the solidifying interface, and Eq. (11) states the fact that the heat liberated at the solidification interface is responsible for a discontinuity in the heat flux at the interface.

III. Solution Methodology

The equations governing the fluid flow in the momentum boundary layer, Eqs. (1) and (2), the flow and heat transfer in the thermal boundary layer, Eqs. (1–3), and the heat transfer in the coating layer, Eq. (4), will be considered sequentially because the solution of the forced convection problem in the liquid region is needed for the solution of the conduction problem in the solid region.

Solution of the Forced Convection Problem

Introducing the stream function in the usual manner

$$u = \frac{\partial \psi}{\partial y} \tag{16}$$

$$v = -\frac{\partial \psi}{\partial x} \tag{17}$$

and the similarity variable and similarity function

$$\xi = \frac{y}{\sqrt{2x}} \tag{18}$$

$$f(\xi) = \frac{\psi}{\sqrt{2x}} \tag{19}$$

we transform Eqs. (2) and (3) to

$$f''' + f f'' = 0 \tag{20}$$

$$T'' + Pr\, f T' = 0 \tag{21}$$

The similarity form of the boundary conditions is

$$f'(\xi_s) = 1 \tag{22}$$

$$f(\xi_s) = \frac{\rho_s}{\rho}\xi_s \tag{23}$$

$$f'(\infty) = \frac{U_\infty}{U_w} \tag{24}$$

$$T(\xi_s) = 1 \tag{25}$$

$$T(\infty) = 0 \tag{26}$$

Note that the value of the similarity variable at the solidifying interface is unknown and will be determined via an iterative process that will be described later.

Solution of the Conduction Problem in the Coating Layer

Utilizing the similarity variable in Eq. (18) we transform the energy equation [Eq. (4)] to

$$T_s'' + PrA\,\xi T_s' = 0 \tag{27}$$

In terms of the similarity variable ξ, the matching conditions [Eqs. (8) and (11)] become

$$\xi_s = \frac{Ste}{PrA}\left[T_s'(\xi_s) + BT'(\xi_s)\right] \tag{28}$$

The boundary conditions for the temperature at the surface of the substrate and at the solidifying interface, respectively, are

$$T_s(0) = 0 \tag{29}$$

$$T_s(\xi_s) = 1 \tag{30}$$

In Eq. (28), a new dimensionless parameter appeared, namely, the ratio of the liquid to the solid thermal conductivity:

$$B = \frac{k}{k_s}\frac{T_w - T_\infty}{T_w - T_f} \tag{31}$$

Integrating Eq. (27) subject to conditions Eqs. (29) and (30) yields

$$T_s(\xi) = \frac{\mathrm{erf}[(PrA/2)^{1/2}\xi]}{\mathrm{erf}[(PrA/2)^{1/2}\xi_s]} \tag{32}$$

Substituting Eq. (32) into Eq. (28), we obtain a simpler expression for ξ_s:

$$\xi_s = \frac{Ste}{PrA}\left[\frac{(2PrA/\pi)^{1/2} e^{-(PrA/2)\xi_s^2}}{\mathrm{erf}[(PrA/2)^{1/2}\xi_s]} - BT'(\xi_s)\right] \tag{33}$$

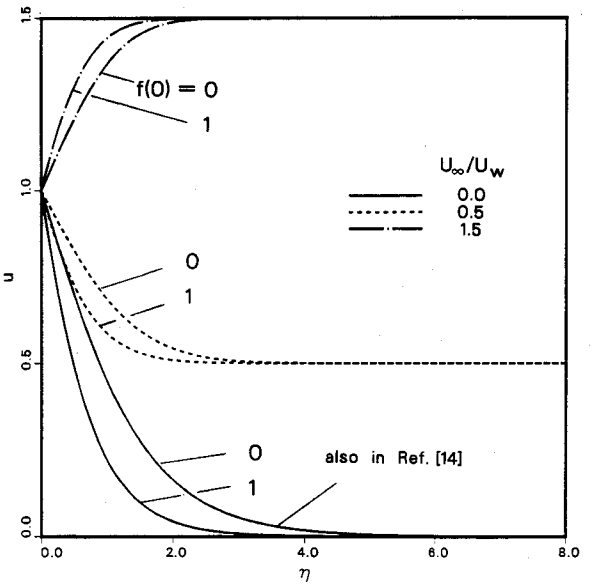

Fig. 2 Effect of the suction velocity at the solidifying interface on the velocity distribution in the boundary layer.

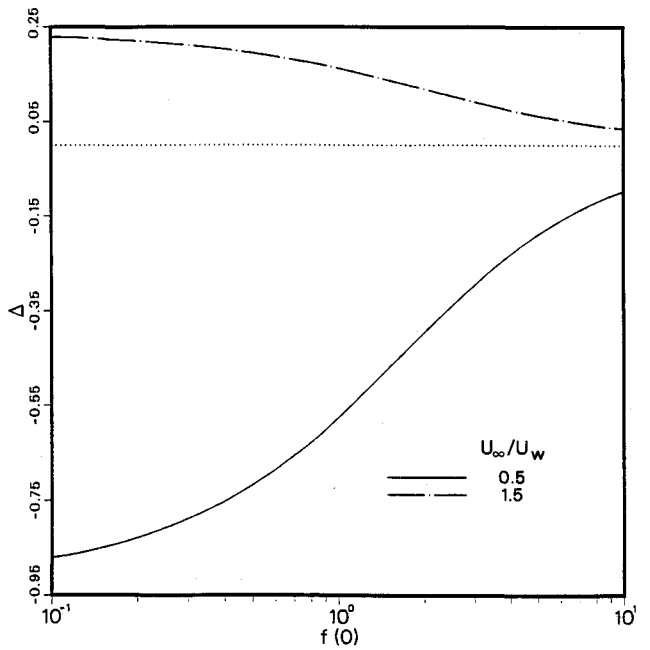

Fig. 3 Effect of the suction velocity at the solidifying interface on the displacement thickness for characteristic values of the velocity ratio.

At this point, the problem formulation in terms of the similarity variables is completed. The solution procedure continues numerically as follows.

1) A value of ξ_s is guessed.

2) Next, the flow part of the convection problem [Eqs. (20) and (22-24)] is solved with the help of a shooting scheme involving the fourth-order Runge-Kutta method for the numerical integration of Eq. (20).

3) With the flowfield known, Eqs. (21), (25), and (26) are solved for the temperature field in the liquid phase with the help of the same numerical scheme used earlier to obtain the solution of the velocity field. Since the temperature field in the liquid phase is now known, the temperature gradient $T'(\xi_s)$ can be evaluated.

4) Finally, the obtained value of $T'(\xi_s)$ is substituted into Eq. (33), and the resulting algebraic equation for ξ_s is solved numerically. If the value that the solution yields for ξ_s matches the guessed value at the beginning of the numerical procedure, the process is terminated. Otherwise, the process is repeated by adjusting the value of ξ_s systematically until the guessed value and the value obtained from Eq. (33) are identical within prescribed error (10^{-4}).

Following this procedure, the effect of the main parameters of the problem on the growth of the coating layer and the heat transfer at the solidifying interface is determined. It is presented in the following section.

IV. Results and Discussion

The discussion of results begins with the presentation of the velocity profiles in the viscous boundary layer. Figure 2 demonstrates the effect of two parameters on the velocity distribution: the suction velocity at the coating/liquid interface $f(\xi_s)$ and the ratio of the freestream velocity U_∞ to the surface velocity in the liquid phase (U_∞/U_w). If the plate velocity is fixed, increasing the freestream velocity such that

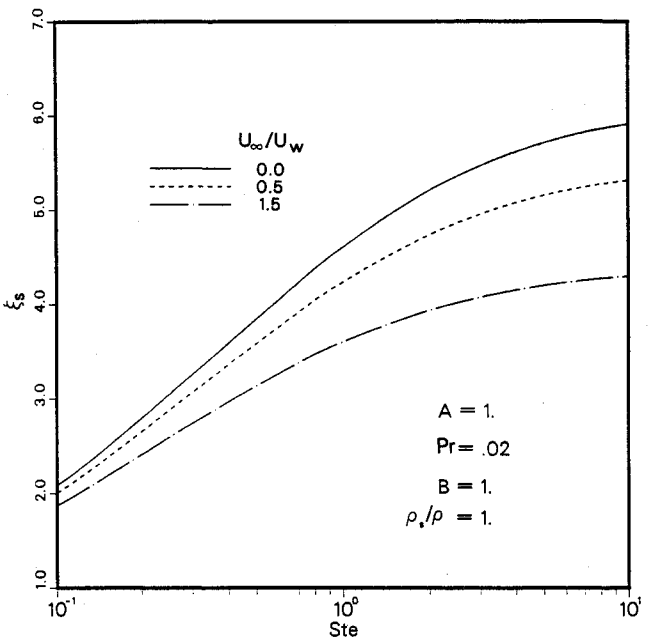

Fig. 4 Effect of the Stefan number on the thickness of the coating layer for characteristic values of the velocity ratio.

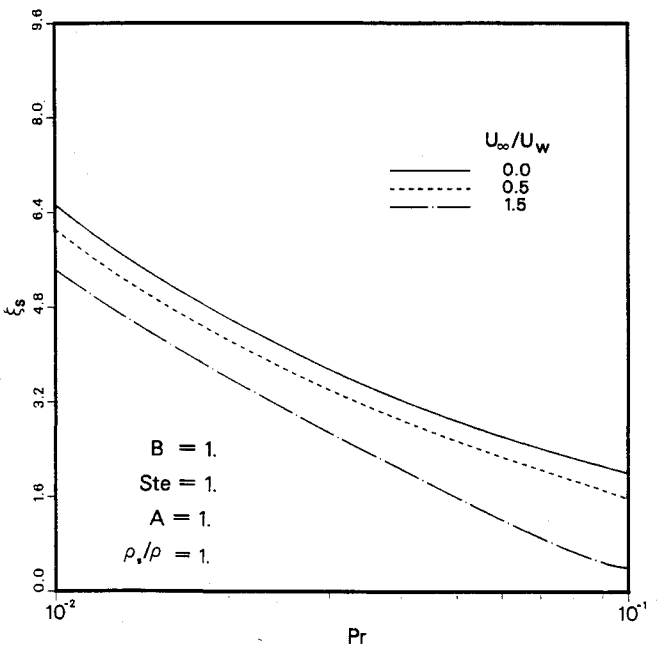

Fig. 5 Effect of the Prandtl number on the thickness of the coating layer for characteristic values of the velocity ratio.

$U_\infty/U_w = 0.5$, 1.5 yields a thinner boundary layer and decreases the magnitude of the velocities inside the boundary layer. The result of increasing the suction velocity caused by the freezing is to obtain a thinner boundary layer for all cases shown in Fig. 2. In the limit of boundary-layer flow over an impermeable moving flat surface, the results of Sakiadis[14] were reproduced accurately.

A quantity of interest is the displacement thickness defined as follows:

$$\Delta = \int_{\xi_s}^{\infty} \left(1 - \frac{U_w}{U_\infty} u\right) dy \tag{34}$$

Physically, the displacement thickness represents the displacement of the external flow because of the presence of the boundary layer. When the freestream velocity is greater than the plate velocity, the outer flow needs to be displaced outward to satisfy continuity relative to the case where the boundary layer does not exist.[15] Therefore, the displacement layer is positive. On the other hand, when the plate velocity is greater than the freestream velocity, the outer flow needs to be displaced inward according to Eq. (34) in order to satisfy continuity relative to the case where the boundary layer does not exist. Therefore, the displacement thickness is negative. In Fig. 3, an example of each of the previous cases is shown. Clearly, regardless of the value of the parameter U_∞/U_w, the effect of the suction caused by the freezing at the solidifying interface is to decrease the absolute value of the displacement thickness. This result makes sense physically and agrees with the findings presented in Fig. 2, where it was shown that the suction caused by the freezing decreases the thickness (and, therefore, the intrusiveness) of the boundary layer.

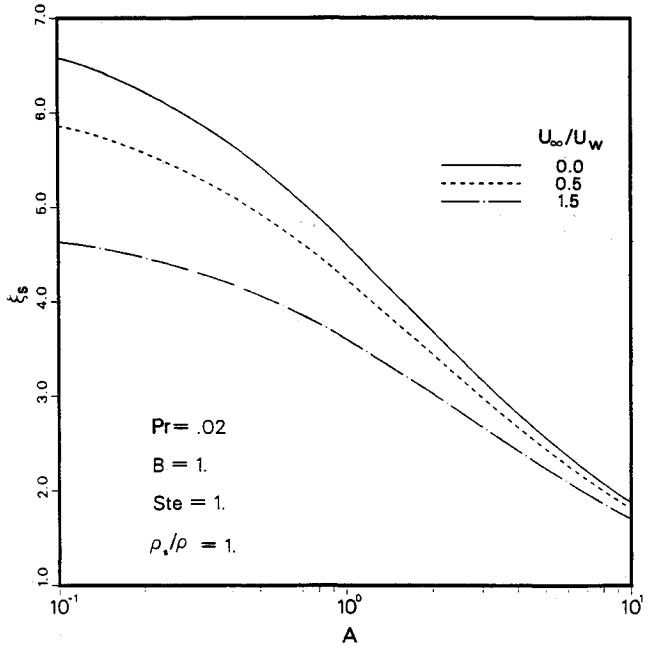

Fig. 6 Effect of parameter A on the coating thickness for characteristic values of the velocity ratio.

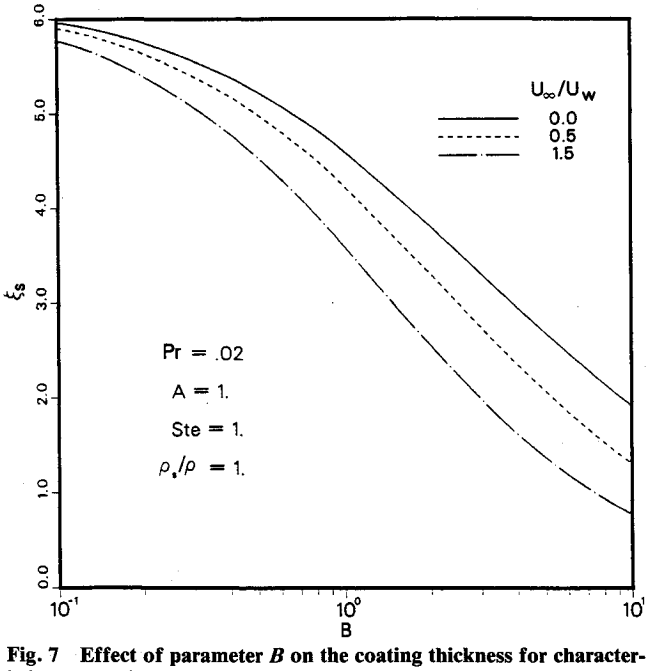

Fig. 7 Effect of parameter B on the coating thickness for characteristic values of the velocity ratio.

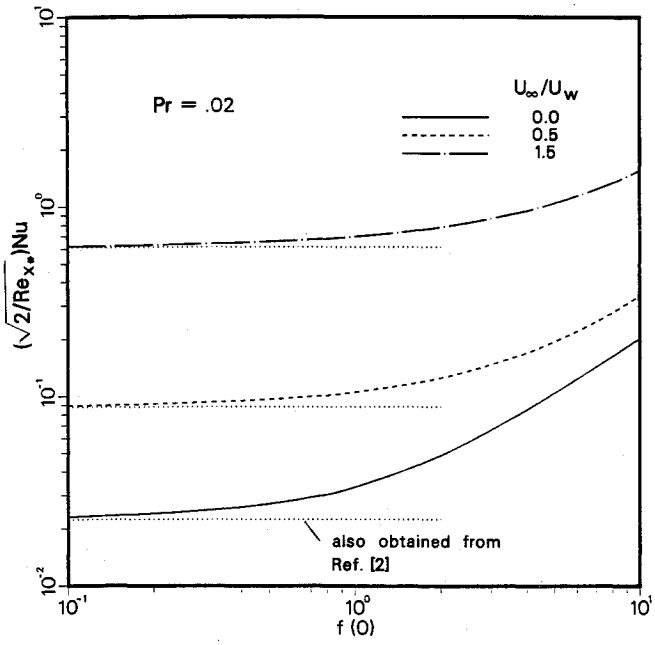

Fig. 8 Effect of the suction velocity caused by the freezing on the heat transfer to the surface.

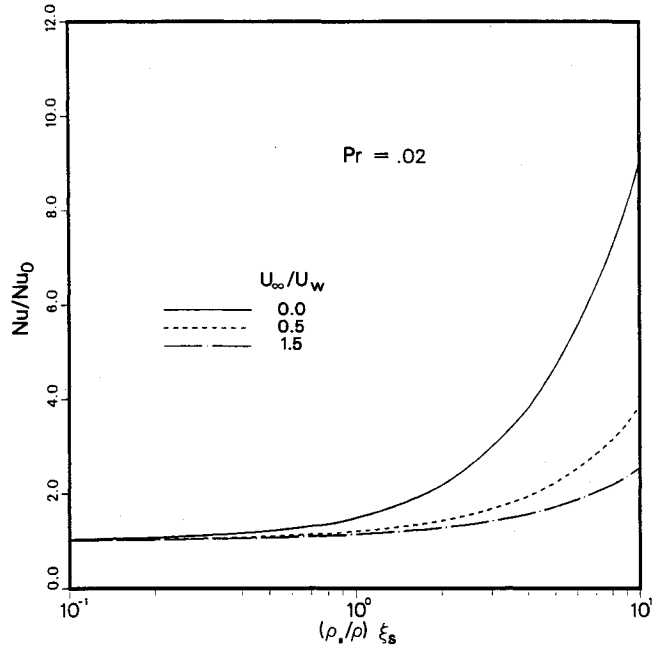

Fig. 9 Effect of the group $(\rho_s/\rho)\xi_s$ on the ratio Nu/Nu_0.

In the sequence of Figs. 4–7, the effect of the major parameters of the problem on the coating thickness, a central part of this study, is presented. Note that the value $\rho_s/\rho = 1$ in Figs. 4–7 corresponds to the situation where there is no suction at the solidifying interface [Eq. (8)]. In Figs. 4–7 it is clear that increasing the value of the ratio U_∞/U_w yields a thinner coating layer. Therefore, the coating thickness can be reduced, if desired, by either increasing the freestream velocity of the deposited material or decreasing the velocity of the moving surface on which the material is deposited. Increasing the value of the Stefan number thickens the coating layer (Fig. 4). This effect weakens at large values of Stefan number. Since, by the definition of the Stefan number [Eq. (15)], for a fixed material, increasing the Stefan number implies the decrease of the surface temperature T_w on which the material is deposited (subcooling effect), this result makes sense physically. Also shown in Fig. 4 is the fact that the impact of the velocity ratio U_∞/U_w weakens as the value of Stefan number decreases.

The effect of increasing the Prandtl number is to decrease the coating thickness (Fig. 5). Note that the range of variation of Pr is applicable to liquid metallic or glassy substances for which this study is pertinent. As shown in Fig. 6, the smaller the thermal diffusivity of a material in the liquid phase is than the thermal diffusivity of the same material in the solid phase, the thicker the resulting coating layer. This effect weakens at very small values of A [$A = 0(10^{-1})$]. An additional observation in Fig. 6 is that increasing A weakens the effect of the velocity ratio U_∞/U_w.

Parameter B, as defined in Eq. (31), can be interpreted directly as representing the ratio of the thermal conductivity of the melt to that of the solid coating if T_w, T_f, and T_∞ are constant. According to Fig. 7, increasing B (or increasing the conductivity of the melt relative to that of the coating layer) decreases the coating thickness. The effect of B is weaker at small values of B. Moreover, the effect of U_∞/U_w weakens as B decreases.

A quantity of engineering interest, in addition to the thickness of the coating layer, is the heat transfer rate at the solidifying interface reported with the help of the Nusselt number:

$$Nu = \frac{-\left(\frac{\partial T_*}{\partial y}\right)_{y=\delta_s} x_*}{(T_f - T_\infty)} = -\left(\frac{dT}{d\xi}\right)_{\xi=\xi_s} \sqrt{\frac{Re_{x_*}}{2}} \tag{35}$$

The effect of the suction caused by the freezing at the solidification interface on the value of Nu is shown in Fig. 8. Clearly, increasing the suction velocity increases the heat transfer at the interface in all cases. As the value of $f(\xi_s)$ decreases, the limit of no freezing at the interface is approached, as shown by the dotted asymptotes. In the limit of $U_\infty/U_w = 0$ (the melt is stationary) and of no freezing at the interface [$f(\xi_s) = 0$], the result of Ref. 2 was reproduced accurately. The effect of the velocity ratio on the heat transfer to the surface becomes more important as the suction velocity at the solidifying interface increases.

The impact of the flow-freezing interaction on the solidification thickness and the heat transfer at the interface is illustrated in Fig. 9. The ratio of the two Nusselt numbers in the ordinate weighs the heat transfer to the surface (Nu) relative to the heat transfer to the surface in the limit of no suction at the solidifying interface (Nu_0), i.e., by neglecting the flow-freezing interaction. Clearly, neglecting the flow-freezing interaction is only acceptable at small values of the group $(\rho_s/\rho)\xi_s (< \approx 0.2)$ for the case of $U_\infty/U_w = 0$. Note that according to Eq. (23) the group $(\rho_s/\rho)\xi_s$ represents the suction velocity at the interface. Increasing the value of the velocity ratio extends the region in which the flow-freezing interaction has a negligible effect on the heat transfer to the surface. For example, for $U_\infty/U_w = 1.5$, according to Fig. 9, the flow-freezing interaction has a marginal impact for up to $(\rho_s/\rho)\xi_s \approx 0.5$. As the value of the group $(\rho_s/\rho)\xi_s$ increases beyond unity, the impact of the flow-freezing interaction increases drastically.

Before closing this section, it is worth stressing that the applicability of the results presented here is limited by the assumption that the moving surface is isothermal. As shown in the Appendix, this assumption is valid if the thermal diffusivity of the body on which the coating is deposited is smaller (in an order of magnitude sense) than the thermal diffusivity of the coating material. When the coating material is a liquid metal or crystal (large thermal diffusivity), it is expected that the isothermality assumption generally will be valid.

V. Conclusions

In this paper, a theoretical solution was presented for the problem of coating a flat moving surface (substrate) with a metallic or glassy (low Prandtl number) melt. It was found that increasing the value of the velocity ratio U_∞/U_w yields a thinner coating layer in all cases. Increasing the Stefan number increased the thickness of the coating layer, whereas increasing the Prandtl number, the ratio of liquid to solid thermal diffusivity (parameter A), and the ratio of liquid to solid thermal conductivity (parameter B) decreased the coating thickness. The convection transport in the melt and the conduction transport in the solid layer were coupled through the suction velocity caused by the freezing at the solidifying interface. Neglecting this coupling is a good approximation only for thin coating layers and for large values of the velocity ratio U_∞/U_w.

From a practical standpoint, the results of the present study identify the trends of the impact of several important controlling parameters (relevant to heat and fluid flow) in the manufacturing of coating layers or the manufacturing of thin metallic or glassy strips.

Appendix

In this Appendix, a scaling analysis is performed that defines the parametric domain of validity of the assumption that the temperature of the surface on which the coating is deposited T_w is constant. A schematic based on which the analysis is performed is shown in Fig. A1.

We begin by considering the case where conduction does take place in the body on which the coating is deposited and where T_w is not necessarily constant. To be consistent with the boundary-layer assumption in the melt and coating, we assume that conduction in the substrate (body) is also of the boundary-layer type ($\delta_* \ll L$). The conduction equation in the coating and the body are

$$\alpha_s \frac{\partial^2 T_{s_*}}{\partial y_*^2} = U_w \frac{\partial T_{s_*}}{\partial x_*} \tag{A1}$$

$$\alpha_b \frac{\partial^2 T_{b_*}}{\partial y_*^2} = U_w \frac{\partial T_{b_*}}{\partial x_*} \tag{A2}$$

For the problem in hand, the scales of the various quantities in Eqs. (A1) and (A2) are

$$\frac{\partial^2 T_{s_*}}{\partial y_*^2} \sim \frac{T_f - \bar{T}_w}{\delta_{s_*}^2}, \qquad \frac{\partial T_{s_*}}{\partial x_*} \sim \frac{T_f - \bar{T}_w}{L}$$

$$\frac{\partial^2 T_{b_*}}{\partial y_*^2} \sim \frac{\bar{T}_w - T_0}{\delta_*^2}, \qquad \frac{\partial T_{b_*}}{\partial x_*} \sim \frac{\bar{T}_w - T_0}{L} \tag{A3}$$

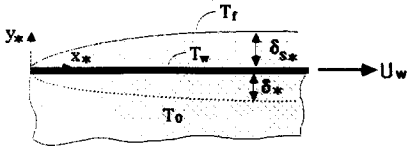

Fig. A1 Schematic for the scaling in the Appendix.

Combining Eqs. (A1–A3) we obtain two scaling statements

$$\frac{\delta_{s_*}}{L} \sim A^{-1/2} Pr^{-1/2} Re_L^{-1/2} \tag{A4}$$

$$\frac{\delta_*}{L} \sim \frac{\alpha_b}{\alpha_s} A^{-1/2} Pr^{-1/2} Re_L^{-1/2} \tag{A5}$$

For the assumption of constant wall temperature to be valid, the following should be true

$$\frac{\delta_*}{\delta_{s_*}} < 0(1) \tag{A6}$$

Substituting Eqs. (A4) and (A5) into Eq. (A6) yields the final criterion necessary for the validity of the T_w = constant assumption:

$$\frac{\alpha_b}{\alpha_s} < 0(1) \tag{A7}$$

Note that liquid metals and liquid crystals often possess large thermal diffusivities. Therefore, Eq. (A7) is, to a large extent, valid within the premises of tbe present study.

Acknowledgment

Support for this work, which was provided by the National Science Foundation through Grant ENG. 84-51144, is greatly appreciated.

References

[1]Flinn, J. E., *Rapid Solidification Technology for Reduced Consumption of Strategic Materials,* Noyes, Park Ridge, NJ, 1985, pp. 29–32.

[2]Kuiken, H. K., "Solidification of a Liquid on a Moving Sheet," *International Journal of Heat and Mass Transfer,* Vol. 20, 1977, pp. 309–314.

[3]Griffin, O. M., "An Integral Energy-Balance Model for the Melting of Solids on a Hot Moving Surface, With Applications to the Transport Processes During Extrusion," *International Journal of Heat and Mass Transfer,* Vol. 20, 1978, pp. 675–683.

[4]Levy, H. L. R. M., Lockyer, A. J., and Arridge, R. G. C., "The Coating of Fibers," *International Journal of Heat and Mass Transfer,* Vol. 21, 1978, pp. 435–443.

[5]Deryagin, B. V., "Theory of the Deposition of a Viscous Liquid onto a Fibre or Wire Being Withdrawn from the Liquid," *Frikl. Mekh. Tekh. Phys.,* Vol. 3, 1963, pp. 71–78.

[6]Anthony, T. R., and Cline, H. E., "A Fluid-Flow-Temperature Model for the Casting of Amorphous Metal Ribbon by Melt Extraction," *Journal of Applied Physics,* Vol. 50, 1979, pp. 239–244.

[7]Zoutendyk, J. A., "Analysis of Forced Convection Heat Flow Effects in Horizontal Ribbon Growth from the Melt," *Journal of Crystal Growth,* Vol. 50, 1980, pp. 83–93.

[8]Seeniraj, R. V., and Bose, T. K., "Freeze-Coating on a Continuous Moving Sheet and on an Axially Moving Cylinder," *Warme-und Stoffubertragung,* Vol. 15, 1981, pp. 239–243.

[9]Cheung, F. B., "Analysis of Freeze Coating on a Nonisothermal Moving Plate by a Perturbation Method," *International Journal of Heat and Mass Transfer,* Vol. 107, 1985, pp. 549–556.

[10]Erickson, L. E., Cha, L. C., and Fan, L. T., "The Cooling of a Moving Continuous Flat Sheet," *Chemical Engineering Symposium Series (Heat Transfer),* AIChE, NY, Vol. 62, 1966, pp. 157–165.

[11]Erickson, L. E., Fan, L. T., and Fox, V. G., "Heat and Mass Transfer on a Moving Continuous Flat Plate With Suction or Injection," *I and EC Fundamentals,* Vol. 5, 1966, pp. 19–25.

[12]Cheung, F. B., "Thermal Boundary Layer on a Continuous Moving Plate With Freezing," *Journal of Thermophysics and Heat Transfer,* Vol. 1, 1987, pp. 335–342.

[13]Cheung, F. B., and Cha, S. W., "Finite-Difference Analysis of Growth and Decay of a Freeze Coat on a Continuous Moving Cylinder," *Numerical Heat Transfer,* Vol. 12, 1987, pp. 41–56.

[14]Sakiadis, B. C., "Boundary-Layer Behavior on Continuous Solid Surfaces: II. The Boundary Layer on a Continuous Flat Surface," *AIChE Journal,* Vol. 7, 1961, pp. 221–225.

[15]John, J. E. A., and Haberman, W. L., *Introduction to Fluid Mechanics,* Prentice-Hall, Englewood Cliffs, NJ, 1988.